

Optical second-harmonic generation from Ag quantum wells on Si(111)7×7: Experiment and theory

Thomas Garm Pedersen, Kjeld Pedersen, and Thomas Brun Kristensen

Institute of Physics, Aalborg University, Pontoppidanstræde 103, DK-9220 Aalborg Øst, Denmark

(Received 1 July 1999)

Optical second-harmonic generation is shown to be an excellent probe of quantization effects in metallic quantum wells. This technique allows *in situ* monitoring of samples during growth in ultrahigh vacuum, and in contrast to linear spectroscopy it is not limited by screening processes. As a practical demonstration, the thickness dependence of the second-harmonic signal recorded during growth of Ag on Si(111)7×7 is presented. The recorded signals show clear oscillations with the film thickness, and the positions of maxima shift towards lower coverage with increasing pump frequency. The essential features of the experimental results are well described by a simple model treating the Ag film as a one-dimensional quantum well. It is demonstrated that excitations from localized quantum well states into states coupled to the Si conduction band continuum are responsible for the main resonances in the nonlinear signal. [S0163-1829(99)52044-4]

Semiconductor quantum well (QW) structures play an increasingly important role in fabrication of new devices such as QW lasers and in fundamental studies of two-dimensional electronic systems (see, e.g., Ref. 1). The unique physical properties of QW's all derive from the quantization of electronic motion along the growth direction, resulting in discrete energy levels. Linear optical spectroscopy allows a direct determination of the discrete level structure and has for this reason emerged as the most important tool for characterization of semiconductor QW's.¹

The degree of quantization can be enhanced significantly if the confinement is produced by a metallic layer rather than a semiconductor. Hence, by confining electrons to thin metallic films grown on a semiconducting or dielectric substrate, a subband splitting of several eV is easily achieved^{2,3} due to the large band offset. Among the available experimental techniques, photoemission^{2,3} and electron tunnelling⁴ have been successfully used as probes of the quantization in metallic QW's. These techniques are limited by their inability to continuously monitor film properties during growth under ultrahigh vacuum (UHV) conditions, however. In view of the success of linear spectroscopy on semiconductor samples, one might expect this technique to be applicable in the case of metallic QW's as well. Moreover, as an all-optical technique it would allow *in situ* monitoring of film growth in UHV. Both experiments⁵ and theory⁶ show, however, that linear optical spectroscopy is unable to resolve discrete resonances, due to the large Drude-like screening in metals. Hence, the obvious solution is to apply *nonlinear* optical spectroscopy, since this technique is much less sensitive to screening but still retains the advantages of linear spectroscopy. Second-harmonic generation (SHG) has previously been applied in studies of semiconductor QW's,⁷ as well as QW states formed in the relative energy gap between the constituents of purely metallic layered structures.⁸ In these works, the fact that the dipole contribution to SHG vanishes in structures with inversion symmetry was used to monitor the effects of symmetry breaking by applied electric⁷ and magnetic⁸ fields, respectively.

In the present work, we wish to demonstrate that second-

harmonic (SH) spectroscopy provides an excellent tool for characterization of metallic QW's formed by depositing an epitaxial layer of metal on a semiconducting substrate. Observation of QW effects requires, however, that the film has little thickness variation along the surface and forms an abrupt interface to the substrate. Ag on Si(111) meets, at least to some extent, these requirements. Room-temperature deposition on the 7×7 reconstructed surface leads to formation of flat islands and a growth mode resembling a two-dimensional layer-by-layer mode.^{9,10} Indeed, QW effects in this system have already been observed in photoemission spectra by Wachs *et al.*,² who demonstrated that the binding energy of discrete occupied states was lowered with increasing film thickness.

Clean surfaces with sharp 7×7 low energy electron diffraction (LEED) patterns were obtained by purely resistive heating of samples cut from a 1-mm-thick wafer with a resistivity of 4.5 Ω cm. Silver was deposited at room temperature from a Knudsen cell and the coverage was determined by a quartz crystal. During deposition, the pressure stayed below 5×10⁻¹⁰ mbar. The films showed 1×1 LEED patterns and atomic force microscopy scans performed after the samples had been taken out into free air, revealed flat triangular domains a few hundred nm wide. SHG measurements were performed using four different pump frequencies obtained from a Q-switched Nd:YAG laser (1.17 and 2.34 eV) and a Ti:sapphire laser (1.40 and 1.70 eV). The SH signals were detected by a photomultiplier tube connected to gated electronics and a quadratic dependence on pump intensity was assured. The results obtained at different frequencies were put into the same scale with the help of a reference signal from a quartz crystal.

Recordings of SHG during growth using a 60° angle of incidence and a *p*-polarized pump and SH light are shown in Fig. 1. The unit used in these curves corresponds roughly to 10⁻²¹ cm²/W. The signals show 3 to 4 maxima in damped oscillations superimposed on the contribution from the substrate, which is important near and above direct interband transitions in Si. As the pump frequency is increased, the

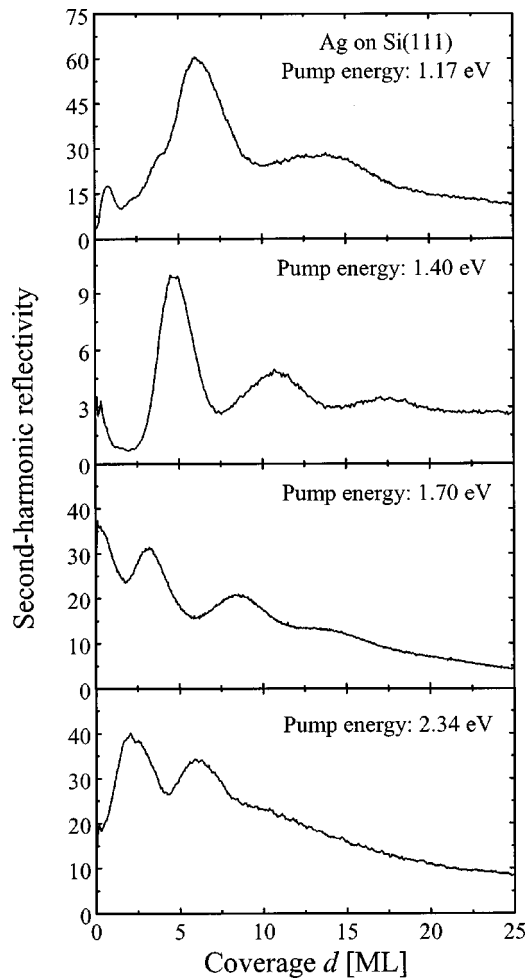


FIG. 1. Measured thickness dependence of SHG from Ag films on Si(111). Results for p to p polarization configuration are shown for four different pump energies.

positions of the maxima shift to lower coverage and the oscillation period decreases. Hence, the manner in which the resonances shift with pump frequency fits the expected behavior of a QW system: As the well thickness grows, the number of bound states increases and the distance between them will decrease. The first resonance will therefore appear at lower coverage when the pump frequency increases. Oscillations in SHG appear as the states go in and out of resonance with the excitation frequency. It is thus clear that the signal will oscillate faster when the pump frequency increases. The oscillations die out for high coverages because the system moves towards a continuum of levels. For the Ag film, it is also known that the roughness increases with coverage^{9,10} leading to variations in the QW thickness along the surface. Therefore, the number of observable oscillations increases with pump frequency also, simply because the period is decreasing. On the other hand, at the highest pump frequency used here (2.34 eV) the SH frequency is in the range where d bands are excited. The tightly bound d electrons are relatively insensitive to the potential barriers introduced by the interfaces, and so their contribution to the nonlinear signal is approximately independent of film thickness. Hence, it is expected that the d bands will add a uniform background to the signal at 2.34 eV. From Fig. 1 it is seen that, indeed, the QW oscillations are best observed at 1.4 and 1.7 eV.

In order to confirm that the resonances in the nonlinear signal correspond to transitions between quantum well states, we have compared the experimental curves to calculations based on a simple model. Obviously, a detailed explanation of the experimental results would require a rather sophisticated model taking into account the surface states of the Si substrate as well as the modification of these states by the Ag layer. In the present work, however, we only wish to demonstrate that the essential features of the thickness dependence, i.e., position and intensity of the maxima, are in fact explained by a highly simplified quantum well description of the Ag layer. Hence, band structure effects are neglected and the electronic states are obtained from a quantum well potential that only varies along the growth direction (z direction). The simplest model which may be imagined for the Ag layer is a symmetric rectangular well. In geometries with inversion symmetry, however, the dipole contribution to the nonlinear response vanishes and the SH signal obtained from such a model will be much too small to account for the experimental curves. A physically reasonable asymmetric potential can be formed by lowering the Ag/Si barrier compared to the Ag/vacuum barrier. If only transitions between localized states inside the well are considered, however, the thickness dependence obtained from such a model will consist of a series of sharp peaks, in contrast to the broad features seen experimentally. In addition, the high barriers tend to produce wave functions which are still approximately symmetric or antisymmetric. Hence, even though a dipole contribution exists in this model, the theoretical response is orders of magnitude less than the measured one. It follows that excitations into quasifree states coupled to the Si conduction band continuum must be taken into account. These states are highly asymmetric since they decay exponentially into the vacuum but oscillate inside the substrate. Furthermore, the continuum of levels formed by these states leads to a broadening of the resonances.

In the actual calculations, the quantum well depth is simply taken as the sum of the bulk Fermi level and the work function (in total, 9.8 eV below vacuum); and the Si level is taken as the conduction band minimum (~ 3.9 eV below vacuum). A smooth Ag/Si interface varying between these levels over a distance of three monolayers is assumed, and on the vacuum side the Ag potential is terminated by the image potential given by $V(z) = e^2/[8\pi\epsilon_0(z-z_0)]$, where $z_0 = 0.73 \text{ \AA}$ is required by continuity (the "floor" of the quantum well extends from $z=0$ to $z=d$). In order to handle the conduction band continuum, the semi-infinite Si substrate is replaced by a 40- \AA slab and the image potential is terminated by a barrier 40 \AA into the vacuum. Once the electronic wave functions (φ_n) and energy eigenvalues (E_n) are determined, the SH signal is obtained from nonlinear response theory.¹¹ At an angle of incidence of $\theta = 60^\circ$, the zzz element of the second order susceptibility is entirely dominating, and consequently all other elements are neglected. In addition, only the z dependence of fundamental (ω) and second harmonic (2ω) fields is retained. This z dependence derives from discontinuities at the boundaries as well as complex phase factors of the form $\exp(\pm iq_\perp z)$, with $q_\perp = (2\pi/\lambda)\sqrt{\epsilon - \sin^2\theta}$, where λ is the vacuum wavelength and ϵ is the dielectric constant of vacuum, Ag or Si. Since z

$\ll \lambda$, such phase factors are replaced by unity. Thus, in the low temperature limit, the effective tensor element χ_{zzz} is given by

$$\chi_{zzz} = \frac{e^3 m_e}{4 \pi \epsilon_0 \hbar^5 \omega^3} \sum_{lmn} \frac{E_{nl} E_{lm} E_{mn}}{2 \hbar \omega + i \hbar / \tau - E_{nm}} \left\{ \frac{H(E_m) - H(E_l)}{\hbar \omega + i \hbar / \tau - E_{lm}} + \frac{H(E_n) - H(E_l)}{\hbar \omega + i \hbar / \tau - E_{nl}} \right\} Z_{nl}^\omega Z_{lm}^\omega Z_{mn}^{2\omega}, \quad (1)$$

where τ is the intraband relaxation time, and $E_{\alpha\beta} = E_\alpha - E_\beta$. In addition, $H(E_\alpha)$ denotes the quantity $(E_F - E_\alpha) \theta(E_F - E_\alpha)$, where $\theta(x)$ is the step function and E_F is the (thickness dependent) Fermi energy, which can be calculated from the charge neutrality condition. Finally, the effective dipole matrix elements are given by

$$Z_{\alpha\beta}^\Omega = \int_{-\infty}^{\infty} \varphi_\alpha(z) \varphi_\beta(z) \int_0^z \epsilon_\Omega^{-1}(z') dz' dz, \quad (2)$$

where $\epsilon_\Omega(z)$ is the z -dependent dielectric constant at frequency Ω . Only the Ag/Si discontinuity is included in $\epsilon_\Omega(z)$, since the wave functions are assumed to be sufficiently well localized outside the Ag/vacuum interface that the Ag value of ϵ_Ω applies throughout this region. In turn, the second-harmonic reflectivity $\eta = I_{2\omega} / (I_\omega)^2$ is calculated from

$$\eta = 2 \omega^2 \sqrt{\frac{\mu_0}{\epsilon_0}} |1 + r_p(\omega)|^4 |1 + r_p(2\omega)|^2 \times \sin^4 \theta \tan^2 \theta |\chi_{zzz}|^2 |L^2(\omega) L(2\omega)|^2, \quad (3)$$

where $r_p(\Omega)$ is the p -polarized reflection coefficient at frequency Ω and $L(\Omega)$ is the local field factor¹² taken as the average between the values for Ag and Si. It should be noted that both the asymmetric potential and the screening of the electric fields lead to broken inversion symmetry. It follows that the quantum well structure may produce a large SH response, even though bulk Ag and Si are both centrosymmetric materials. In fact, the calculated response is rather sensitive to the linear dielectric properties and, hence, an important point is that the dielectric constant of an ultrathin Ag layer cannot be expected to resemble the bulk value. First, transitions between size quantized states contribute to the linear response. Secondly, the relaxation time, which also enters in Eq. (1), decreases in thin films due to surface scattering. For simplicity, the former of these contributions is neglected in the present work. A thickness dependent relaxation time can be incorporated, however, by splitting the bulk dielectric constant into inter- and intraband parts, and subsequently obtain a corrected value of the intraband contribution using the Drude expression for the τ dependence.¹³ It should be noted that the Drude expression is rigorously valid even in mesoscopic metallic structures,¹¹ provided the local electron density is used. For simplicity, the local density is approximated by the average one, i.e., the bulk density, below. In addition, the thickness (d) dependence of the relaxation time is obtained from a fitting procedure giving the result (in eV): $\hbar/\tau(d) = 0.10 + 0.2 \exp(-d/35 \text{ \AA}) + 0.8 \exp[-(d/12 \text{ \AA})^2]$.

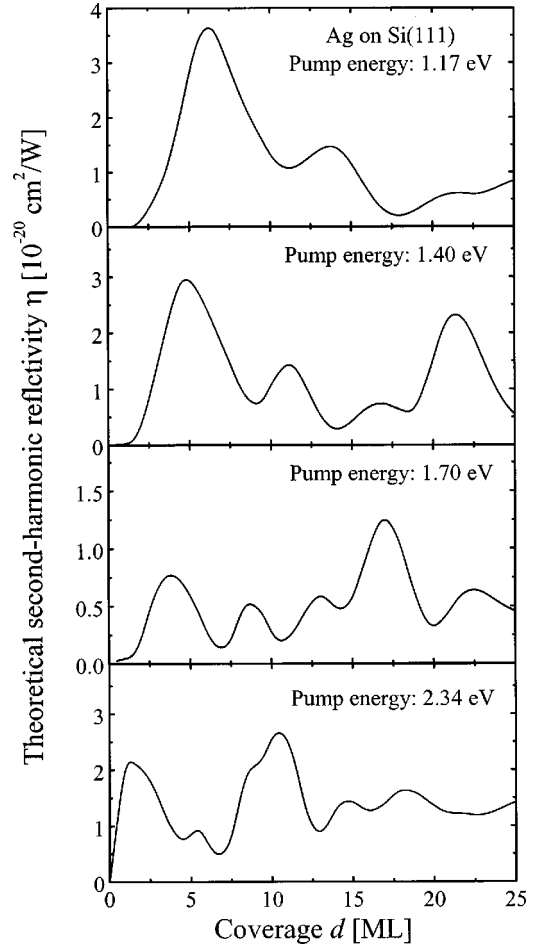


FIG. 2. Calculated SH reflectivity as a function of film coverage.

The above framework presents a simple but realistic description of the SH response of a metallic quantum well. Since all contributions related to the substrate are left out, however, the theory cannot be expected to reproduce the background signal seen in the experimental curves. Furthermore, the calculated response is meaningful only when the thickness d equals an integer number of monolayers, whereas the experimental response is measured as a function of a continuously varying coverage. In fact, the experimental coverage is a measure of the mean thickness, and in order to directly compare experimental and theoretical results, the thickness distribution is needed. For simplicity, a binomial distribution is used and the increasing surface roughness with thickness^{9,10} is incorporated by assuming a linear dependence between the variance σ^2 and d of the form $\sigma^2 = 0.05 \text{ \AA} d$ is assumed.

In Fig. 2, the calculated values of the SH reflectivity η versus mean thickness d are shown. These curves are obtained by averaging the results for integer monolayer coverages given by Eq. (3) using the procedure described above. The calculated curves are seen to be in reasonable agreement with the experimental ones. Clearly, the measured QW signal is superimposed on an exponentially decaying contribution from the substrate when the SH photon energy exceeds the direct Si band gap. However, the location of the calculated maxima is in almost perfect agreement with the experimental results, which demonstrates the validity of the quan-

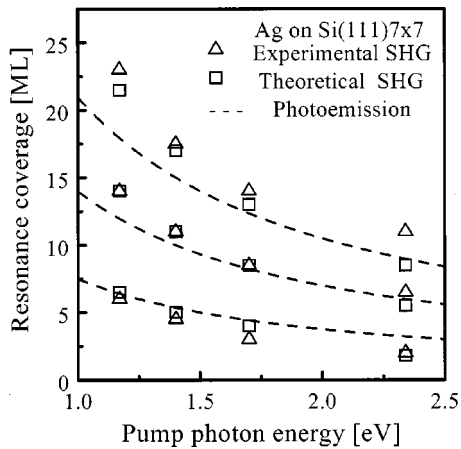


FIG. 3. Comparison between experimental and theoretical resonance coverages as a function of pump photon energy. In addition, fits to photoemission data (Ref. 2) are shown as dashed lines.

tum well model. The relative height of the maxima agrees reasonably well with the experimental trend, except for the fourth peak which is obviously too large. A direct comparison of the experimental and theoretical maxima in SHG is shown in Fig. 3, in which the positions of the maxima are plotted as a function of the pump frequency. The calculated results clearly reproduce the shift of the resonances towards lower coverage with increasing frequency. The intensity of the calculated maxima is rather sensitive to the parameters of the model whereas their location remain approximately fixed.

As an additional test, the resonance positions can be compared to the photoemission data of Wachs *et al.*² While SHG

probes the difference in energy between empty and occupied levels, photoemission directly detects the positions below the Fermi energy of the bound states. For thick films, the bottom of the Si conduction band is expected to be ~ 0.4 eV above E_F . As discussed above, the calculations show that SHG originates from transitions between bound QW levels and the continuum of empty levels in the Si conduction band. The resonance energies observed in SHG are thus expected to be comparable to the binding energies observed in photoemission. The binding energies obtained by Wachs *et al.* were found to vary linearly with the inverse of the film thickness. Curves representing fits of such a relation to the data in Ref. 2 are plotted as dashed curves in Fig. 3, using the same energy scale as for the photon energy. It is seen that the shift of the SH resonances follows the shift of the bound levels quite well. This strongly supports the conclusion that the main resonances in SHG are caused by transitions between localized QW states and the Si conduction band continuum.

In conclusion, it has been demonstrated that SHG is a very sensitive probe of QW states in thin metal films. QW effects are directly observable as oscillations in SHG versus film thickness, without performing any of the data processing frequently applied in other techniques. By comparing the data to calculations of SHG from the QW system, it has been shown that the resonances in SHG are caused by transitions from confined QW states, to states coupled to the Si conduction band continuum. The agreement with experimental results, obtained with a relatively simple theoretical model, is encouraging for further studies of strongly confined electronic systems formed in metal films on semiconductors.

The authors acknowledge the technical assistance of Dr. Brian Vohnsen and the financial support of the Danish Natural Science Council under Grant No. 9502518.

¹C. Weisbuch and B. Vinter, *Quantum Semiconductor Structures. Fundamentals and Applications* (Academic Press, New York, 1991).

²A. L. Wachs, A. P. Shapiro, T. C. Hsieh, and T. C. Chiang, *Phys. Rev. B* **33**, 1460 (1986).

³L. Haderbache, P. Wetzel, C. Pirri, J. C. Peruchetti, D. Bolmont, and G. Gewinner, *Thin Solid Films* **184**, 365 (1990).

⁴R. C. Jaklevic, J. Lambe, M. Mikkor, and W. C. Vassel, *Phys. Rev. Lett.* **26**, 88 (1971).

⁵J. Dryzek and C. Czaplá, *Phys. Rev. Lett.* **58**, 721 (1987).

⁶Y. Silberberg and T. Sands, *IEEE J. Quantum Electron.* **28**, 1663 (1992).

⁷M. M. Fejer, S. J. B. Yoo, R. L. Byer, A. Harwit, and J. S. Harris, *Phys. Rev. Lett.* **62**, 1041 (1989).

⁸A. Kirilyuk, Th. Rasing, R. Megy, and P. Beauvillain, *Phys. Rev. Lett.* **77**, 4608 (1996).

⁹G. Meyer and K. H. Rieder, *Surf. Sci.* **331-333**, 600 (1995).

¹⁰K.-H. Park, J. S. Ha, S.-J. Park, and E. H. Lee, *Surf. Sci.* **380**, 258 (1997).

¹¹O. Keller, *Phys. Rev. B* **33**, 990 (1986).

¹²Y. R. Shen, *The Principles of Nonlinear Optics* (Wiley, New York, 1984).

¹³Y. Borenstein, R. Alameh, and M. Roy, *Phys. Rev. B* **50**, 1973 (1994).